frontiers in Earth Science

ORIGINAL RESEARCH
published: 30 September 2020
doi: 10.3389/feart.2020.564783

A Simplified Classification of the Relative Tsunami Potential in Swiss Perialpine Lakes Caused by Subaqueous and Subaerial Mass-Movements

Michael Strupler[1], Frederic M. Evers[2], Katrina Kremer[1], Carlo Cauzzi[1], Paola Bacigaluppi[2], David F. Vetsch[2], Robert M. Boes[2], Donat Fäh[1], Flavio S. Anselmetti[3] and Stefan Wiemer[1]*

[1] Swiss Seismological Service (SED), Swiss Federal Institute of Technology Zurich, Zurich, Switzerland, [2] Laboratory of Hydraulics, Hydrology and Glaciology (VAW), Swiss Federal Institute of Technology Zurich, Zurich, Switzerland, [3] Institute of Geological Sciences and Oeschger Centre for Climate Change Research, University of Bern, Bern, Switzerland

OPEN ACCESS

Edited by:
Finn Løvholt, Norwegian Geotechnical Institute, Norway

Reviewed by:
Emily Margaret Lane, National Institute of Water and Atmospheric Research (NIWA), New Zealand
Jia-wen Zhou, Sichuan University, China
Carl Bonnevie Harbitz, Norwegian Geotechnical Institute, Norway

***Correspondence:**
Michael Strupler
michael.strupler@sed.ethz.ch

Specialty section:
This article was submitted to Geohazards and Georisks, a section of the journal Frontiers in Earth Science

Received: *22 May 2020*
Accepted: *24 August 2020*
Published: *30 September 2020*

Citation:
Strupler M, Evers FM, Kremer K, Cauzzi C, Bacigaluppi P, Vetsch DF, Boes RM, Fäh D, Anselmetti FS and Wiemer S (2020) A Simplified Classification of the Relative Tsunami Potential in Swiss Perialpine Lakes Caused by Subaqueous and Subaerial Mass-Movements. Front. Earth Sci. 8:564783. doi: 10.3389/feart.2020.564783

Historical reports and recent studies have shown that tsunamis can also occur in lakes where they may cause large damages and casualties. Among the historical reports are many tsunamis in Swiss lakes that have been triggered both by subaerial and subaqueous mass movements (SAEMM and SAQMM). In this study, we present a simplified classification of lakes with respect to their relative tsunami potential. The classification uses basic topographic, bathymetric, and seismologic input parameters to assess the relative tsunami potential on the 28 Swiss alpine and perialpine lakes with a surface area >1 km^2. The investigated lakes are located in the three main regions "Alps," "Swiss Plateau," and "Jura Mountains." The input parameters are normalized by their range and a k-means algorithm is used to classify the lakes according to their main expected tsunami source. Results indicate that lakes located within the Alps show generally a higher potential for SAEMM and SAQMM, due to the often steep surrounding rock-walls, and the fjord-type topography of the lake basins with a high amount of lateral slopes with inclinations favoring instabilities. In contrast, the missing steep walls surrounding lakeshores of the "Swiss Plateau" and "Jura Mountains" lakes result in a lower potential for SAEMM but favor inundation caused by potential tsunamis in these lakes. The results of this study may serve as a starting point for more detailed investigations, considering field data.

Keywords: classification, lake tsunami, subaqueous mass movements, subaerial mass movements, earthquakes, perialpine lakes

INTRODUCTION

Background

Historical reports and recent studies have shown that tsunamis do not only occur in the ocean, but also in lakes where they may cause large damages and casualties. The cause for the displacement of large amounts of water can be due to a large variety of triggers, including subaqueous and subaerial mass-movements (SAQMM and SAEMM, respectively) triggered by earthquakes. The occurrence of tsunami events within Swiss lakes of various size and depths is documented in several reports (**Table 1**).

TABLE 1 | Characteristics of the Swiss lakes with surface areas >1 km (reservoirs excluded), sorted by lake area. Information extracted from swisstopo data.

Index	Name	Lake level (m.a.s.l.)	Maximum depth (m)	Shoreline length (km)[a]	Lake area (km^2)[a]	Historical tsunami year and height (m)	Trigger (SAEMM/SAQMM)
1	Lake Geneva	372	310	229.7	580	AD 563: 8–13 m (Kremer et al., 2012)	SAEMM triggered SAQMM (cascading effect)
2	Lake Constance	395	252	340	539.8	AD1720: "Unusual wave action" (Gisler and Fäh, 2011)	SAQMM (earthquake-triggered)
3	Lake Maggiore	193	372	214.1	215.6		
4	Lake Neuchatel	429	276	140.8	215.2		
5	Lake Lucerne	434	214	157.7	113.9	AD 1601: 3–4 m (Cysat, 1969)	SAQMM (earthquake-triggered)
						AD 1687: >5 m (Hilbe and Anselmetti, 2014 and references therein)	SAQMM
						AD 1931: 3.15 m Alpnachersee (Huber, 1982)	SAEMM
						AD 1982: 2–3 m Kehrsiten (Huber, 1982)	SAEMM
						AD 1982: 3–4 m Gersau (Huber, 1982)	SAEMM
						AD 1963: 4 m Obermatt (Huber, 1982)	SAEMM
						AD 1964: 15 m Obermatt (Huber, 1982)	SAEMM
						AD 2007: 5–6 m Obermatt, 1–1.5 m Weggis (Fuchs and Boes, 2010)	SAEMM
6	Lake Zurich	406	136	136.8	88.9		
7	Lake Lugano	271	288	100.1	49.2		
8	Lake Thun	558	215	63.4	47.8		
9	Lake Biel	429	74	50.2	41.2		
10	Lake Zug	413	197	43.3	38.4		
11	Lake Brienz	564	260	37.5	29.8	AD 1996: "Small tsunami wave" (Girardclos et al., 2007)	SAQMM
12	Lake Walen	419	150	39.4	24.1	AD 1946: 5–6 m (Huber 1982)	SAEMM
						AD 1924: 8–9 m (Huber 1982)	SAEMM
13	Lake Murten	429	46	24.9	22.7		
14	Lake Sempach	504	87	20.2	14.4		
15	Lake Hallwil	449	47	19.7	10.2		
16	Lake Joux	1,004	32	24.9	8.8		
17	Lake Greifen	435	34	17.3	8.3		
18	Lake Sarnen	468	52	17	7.4		
19	Lake Aegeri	724	82	16.1	7.3		
20	Lake Baldegg	463	66	13	5.2		
21	Lake Sils	1,797	71	14.8	4.1		
22	Lake Silvaplana	1,790	77	13.2	3.2		
23	Lake Kloental	844	45	12.5	3.1		
24	Lake Pfaeffikon	537	36	9.2	3.1		
25	Lake Lauerz	447	13	11.5	3	~15 m (Bussmann and Anselmetti, 2010 and references therein)	SAEMM triggered SAQMM (cascading effect)
26	Lake Lungern	688	68	10.5	2		
27	Lake Poschiavo	962	84	7.4	2		
28	Lake Oeschinen	1,578	56	5.5	1.2		

SAEMM, Subaerial mass movements; SAQMM, subaqueous mass movements.

[a]Only the outer shoreline from the SwissTLM3D (swisstopo) dataset (i.e., no shorelines of islands) are considered. This affects also the calculation of the lake area (i.e., land areas of islands not subtracted). Note: only documented mass-movements with wave height estimates are listed.

A well investigated example in Lake Lucerne with wave run-up heights of 3–4 m triggered by SAQMM is the 1601 event assigned to the Mw ~ 5.9 Unterwalden earthquake (Siegenthaler et al., 1987; Schnellmann et al., 2002; Monecke et al., 2004; Fäh et al., 2011). Another documented example is a tsunami (run-up > 5 m) triggered by a spontaneous river delta collapse in Lake Lucerne in 1687 (Siegenthaler and Sturm, 1991; Hilbe and Anselmetti, 2014; Hilbe and Anselmetti, 2015). A more recent event of a rockfall-triggered tsunami (also called impulse-wave) has been reported by Fuchs and Boes (2010): On July 20, 2007, a SAEMM with a total volume of 35,000 m^3 occurred in multiple phases at a closed quarry that is located directly at the shore. The resulting waves with observed heights between 1 and 1.5 m caused some damage at the opposite lake shore (~3.5 km away from the tsunami source). Fuchs and Boes (2010) estimated the maximum wave height close to the tsunami source to 5–6 m (**Table 1**). Shore collapses, mostly triggered by human activity in the past ~150 years, have also been responsible for triggering impulse waves on many Swiss lakes (Huber, 1980; Huber, 1982 and references therein). In addition to single mechanisms identified as tsunami triggers, cascading effects have also caused tsunamis, such as in the case of the "Rossberg" subaerial landslide that mobilized soft sediments on a swamp plane laterally, which, in turn caused a tsunami with an estimated wave height of ~15 m on Lake Lauerz in 1806 AD (Bussmann and Anselmetti, 2010). Similarly, in Lake Geneva, a subaerial rockfall is assumed to have triggered a partial collapse of the Rhone Delta, which led to the 563 AD tsunami with modeled wave heights of ~8 m arriving at the city of Geneva (Kremer et al., 2012).

Next to historically documented lacustrine tsunamis on Swiss lakes, geophysical (i.e., bathymetric and seismic reflection data) and sedimentological data (i.e., sediment cores retrieved at the bottom of several lakes) show evidence of large SAQMM and SAEMM that have occurred since de-glaciation, and many of them are assigned to earthquakes as triggers (e.g., Schnellmann et al., 2002; Monecke et al., 2004; Fanetti et al., 2008; Hilbe et al., 2011; Wirth et al., 2011; Strasser et al., 2013; Corella et al., 2014; Kremer et al., 2015; Reusch, 2015; Fabbri et al., 2017; Kremer et al., 2017; Strupler et al., 2018a).

Potential lake tsunamis resulting from mass-movements as well as the tsunami hazard to date can only be estimated with models. Case studies on tsunamis triggered by SAEMM and SAQMM exist for selected sites in specific lakes (Fuchs and Boes, 2010; Hilbe and Anselmetti, 2015; Strupler et al., 2018c). These studies indicate clearly that there is a potential for future tsunamis on Swiss perialpine lakes. As detailed assessments of the tsunami hazard caused by mass movements require the acquisition of vast amounts of high-resolution geophysical and geological data, it is important to make a preselection of the lakes to be investigated, before evaluating the tsunami potential on a specific lake in detail and with considerable costs. The main aim of this study is therefore to classify all Swiss lakes >1 km^2 (engineered reservoirs excluded) according to their relative tsunami potential caused by SAQMM and SAEMM. Results of such a rapid classification will be used to prioritize lakes for a detailed data acquisition and numerical modeling. Lakes with a relatively low tsunami potential can then be excluded from further analyses. In the following paragraphs, an overview about characteristics of tsunamis that are triggered by SAQMM and SAEMM is given. In the term "mass movements," we include both landslides and rockfalls.

Tsunami Generation by SAEMM

Due to the alpine and perialpine environment, several Swiss lakes are surrounded by steep slopes that may trigger SAEMM. Volumes of reported SAEMM in Swiss lakes have been mostly in the range between a few 1′000 to 1 million m^3 (Huber, 1980). Impulse waves generated by SAEMM have been extensively studied for decades with hydraulic scale-model experiments (Hager and Evers, 2020). Compared to field surveys in the aftermath of an event, where only maximum run-up heights may be tracked along the shores (Roberts et al., 2013), this approach allows for measuring wave characteristics under controlled laboratory conditions (Heller et al., 2008; Evers et al., 2019b). Among the experimental studies conducted in 2D wave channels, Heller and Hager (2010) covered the most extensive range of experimental parameters, including slide volume, slide density, slide thickness, slide porosity, slide impact velocity, slide impact angle, and still-water depth. The slide impact velocity, slide thickness, slide mass, and slide impact angle were found to be the governing 2D parameters: Generally, greater slide impact velocities and masses, i.e., slide volumes for constant slide density, as well as flat impact angles, lead to larger wave heights. Considering a simple block slide model as proposed by Körner (1976), the slide impact velocity is mainly controlled by the drop height, the slope angle, the dynamic bed friction angle, and the gravitational acceleration. A maximum wave height therefore requires an optimal balancing between impact velocity and impact angle when all other slide parameters are considered constant. Heller and Hager (2014) identified a slide impact angle of 51.6° to provide the best conditions for efficient wave generation on a constantly inclined slope. A vertical impact of a SAEMM leads to smaller waves compared to the optimal slide impact angle, due to a less efficient slide to wave energy transfer. Considering only the parameters imposed by the topography, large drop heights and steep slope angles induce high slide velocities. Based on experiments in a wave basin, Evers et al. (2019a) found the slide width to be an additional governing parameter for 3D wave generation and propagation: The wider a slide, the larger the wave.

Tsunami Generation by SAQMM

SAQMM include subaqueous landslides and delta collapses. The occurrence of SAQMM is mainly dependent on a favourable topography, a necessary amount of sediments, and a trigger mechanism (Nadim et al., 1996). Previous work on Swiss lakes has shown that most documented landslides occur on slopes with inclinations between ~10 and 25° (Schnellmann et al., 2006; Hilbe et al., 2011;

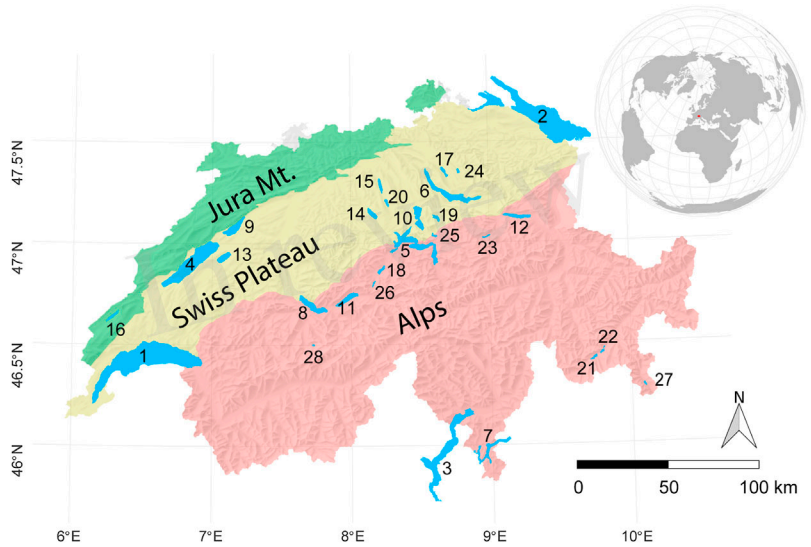

FIGURE 1 | Location of the Swiss (non-reservoir) lakes with surface areas <1 km. Labels refer to **Table 1**. Geodata used with permission from swisstopo.

Strasser et al., 2011; Strupler et al., 2018b). Many of these slides are initiated within a weak layer at the transition from Late Glacial to Holocene sediments (e.g., Strasser et al., 2007; Strasser et al., 2011; Strupler et al., 2017). To date, the yet unfailed lateral slopes of the investigated lakes are covered with a ~3–10 m of potentially mobile, Holocene sediment drape.

Important properties of SAQMM to estimate the characteristic amplitude of resulting waves (i.e., directly above the landslide source area) are the landslide volume, the landslide acceleration, and the submergence depth of the centroid of the landslide below lake level (Watts et al., 2005; Tappin et al., 2008). Generally, a larger slide volume leads to larger wave amplitudes, and a greater central submergence depth of a landslide leads to smaller wave amplitudes.

The basin depth can have an influence on the wave amplitude during generation, as the amplitude is also dependent on the Froude number *Fr* [i.e., ratio between landslide velocity *u* and the shallow-water wave celerity *c* (Løvholt et al., 2015; Glimsdal et al., 2016, **Eq. 1**)],

$$Fr = \frac{u}{c}. \tag{1}$$

Slides that move at velocities close to the shallow-water wave celerity (i.e., $Fr \approx 1$) will generally increase the wave amplitudes (Ward, 2001).

Tsunami propagation and Inundation

After its generation, the wave will propagate across the basin. Dispersion (i.e., the spreading of energy due to different wave celerities for waves with different wavelengths) can cause wave trains that change their shape with distance from the tsunami source and the geometry of the water body (e.g., Glimsdal et al., 2013; Evers et al., 2019b).

In zones where the wave amplitudes are much smaller and the wavelengths are much larger than the stillwater depth *h*, the tsunami propagation velocity *c* can be modeled with the linear shallow water theory:

$$c = \sqrt{gh}. \tag{2}$$

In very narrow valleys, the wave cannot spread radially. During propagation into shallow areas in proximity of shores, the wave develops an increased surface elevation (due to shoaling) and can have devastating effects onshore (e.g., Hafsteinsson et al., 2017).

Existing Approaches for Comparing Tsunami Hazard

Different approaches for comparing the tsunami hazard on multiple lakes and fjords exist. Romstad et al. (2009) conducted a geospatial assessment of the relative rockslide-induced tsunami hazard for Norwegian lakes larger than 0.1 km^2 by calculating a (tsunami-generating) topographic rock slide potential for 18,976 lakes. They assume that all subaerial cells with slope inclinations larger than 30° are potential landslide-release cells, and that only landslides with volumes >5,000 m^3 entering a lake causes a tsunami, based on empirical knowledge and numerical simulations. The volumes of the potential landslides possibly reaching the lake are estimated from an empirical relationship involving the required mobility of each cell, which is represented by a head to horizontal distance of a travel path ratio. Hermanns et al. (2012, 2013) propose a hazard and risk classification system for large unstable rock slopes, which includes structural site investigations and analysis of the activity of the slopes. Based on this classification methodology, Hermanns et al. (2016) classify 22 mapped rock slopes and do i) a volume computation, ii) run-out assessments, iii) assessment of possible wave propagation and run-up if a rockfall enters a water body, and iv) an estimation of people exposed to rock avalanches and rockfall-induced tsunami waves. The results of these studies build on multiple years of systematical mapping of unstable rock-slopes and are to be used as support tool for risk management.

In contrast to these studies, our goal is to estimate the relative tsunami potential on peri-alpine lakes that is caused both by

TABLE 2 | Overview of the input parameters used for the classification of the tsunami potential (before normalization).

Input parameter	Represented by	Main assumption
IP1: Potential for subaerial mass-movements	Ratio of Fahrböschung >30° to total watershed area for each lake	Ratio of area within watershed with Fahrböschung >30° to total watershed area is an indicator of subaerial mass-movement caused tsunami potential, as subaerial rocks tend to mobilize for Fahrböschung >30°
IP2: Potential for subaqueous mass-movements	Ratio of slope area within 10–25° to total slope area. Slope area is defined as all zones with inclinations >5°	Most sublacustrine mass movements occur on slopes with inclinations between 10 and 25°
IP3: Potential for seismicity	Expected SA(0.3s) for earthquakes with an exceedance probability of 10% in 50 years from Wiemer et al. (2016) for each lake center point	Lakes located in zones with greater seismic activity are expected to experience more earthquake-triggered subaerial and subaqueous mass movements
IP4: Inverse SDR	1/"SDR" (Aronow, 1982): Inverse of the actual shoreline length divided by a hypothetical shoreline length for a perfect circle with the actual lake area	The more complex a lake shape (i.e., the larger the ratio between the actual shoreline and the hypothetical shoreline length for a perfect circle), the lower the general tsunami potential on the whole lake. This is assumed as for complex lakes with many basins only a few basins may be affected
IP5: Potential for inundation	Low-lying shore zones. Ratio of zones below lake level up to <5 m above mean lake level within 1,000 m shore-strip around shoreline to total area of 1,000 m shore-strip	Lakes surrounded by a greater percentage of low-lying areas can be affected by larger inundated areas

SDR, shoreline development ratio.

SAEMM and SAQMM. In this study, we do not aim at including site-specific field measurements. Rather, we conduct a desktop analysis of the tsunami potential and the related consequences, based on parameters that are derived mainly from previous studies on peri-alpine lakes. In contrast to the workflow of Strupler et al. (2019), that estimates the location and characteristics of potential SAQMM within a specific peri-alpine lake basin, the methodology presented uses a country-level scale, comparing the tsunami potential on various lakes.

Regional Setting

In Switzerland, a total of 28 lakes with surface areas greater than 1 km^2 (engineered reservoirs excluded) exist (**Figure 1**; **Table 1**). Of these lakes, Lake Geneva has the largest surface area (~580 km^2), while Lake Maggiore has the greatest water depth (372 m). Four of the lakes share borders with neighboring countries, i.e., France (Lake Geneva), Germany, and Austria (Lake Constance), and Italy (Lakes Maggiore and Lugano). Of the investigated lakes, 14 are located in the Alps, 13 on the Swiss Plateau, and one in the Jura Mountains. The origin of these lakes is related to subglacial erosion as they represent glacial overdeepenings. Since de-glaciation after the Last Glacial Maximum, deposition of sediments has been ongoing in the lake-basins.

The lakes with the largest surface area are found in the "Swiss Plateau" region, which is geologically formed by sediments from the Molasse basin and which is characterized by a relatively smooth topography. The "Swiss Plateau" is the region in Switzerland with the highest population density (e.g., Henriod et al., 2016).

Geologically, the Central and Southern Alps consist mainly of crystalline rocks, the Northern Alps of limestones and marls, and the Molasse basin consists mainly of conglomerates and sandstones. The Jura mountains are rich in limestones.

It is estimated that earthquakes with a magnitude 6 or greater are expected to occur every 50–150 years in Switzerland (Wiemer et al., 2016). The highest earthquake hazard can be found in the regions Valais, Basel, and Grisons. Earthquakes in these regions are generally a result of the collision between the European and African plates.

METHODOLOGY AND DATA

General Methodology and Data

In the following, a methodology for the classification of the tsunami potential is presented and applied to Swiss lakes with surface areas greater than 1 km^2 (engineered reservoirs excluded). The automated workflow is implemented in R (R Core Team 2018). Geospatial operations are either conducted directly in R or calculated in ArcGIS, which can be steered from within R using the package "RPyGeo" (Brenning et al., 2018).

First, five input parameters (IP1–IP5; **Table 2**) contributing to the tsunami potential are calculated for each lake. These parameters are discussed in detail in *Parametrization* below. After their calculation, the parameters are normalized by their range (*Normalization of the Input Parameters*). In general, a larger input value means a larger contribution to the tsunami potential. Next, a classification of investigated lakes, according to

their potential for SAEMM (IP1) and SAQMM (IP2) is conducted. Shorelines used in the workflow are taken from SwissTLM3D (swisstopo). Only the outer shorelines are considered, shorelines of islands in lakes are not considered. As topographic elevation model, SRTM (Shuttle Radar Topography Mission) data is used (Jarvis et al., 2008). The dataset has a spatial resolution of 90 m and is used due to the data availability also alongshore border lakes in non-Swiss territory. For a large part of the investigated lakes, high-resolution digital bathymetric datasets SwissBATHY3D (swisstopo) are available. For various lakes, however, bathymetric data has to be interpolated from isobaths (SwissMap Vector 10/25 data; swisstopo). For comparability reasons, both datasets are resampled to a grid resolution of 20 m.

Parametrization

Five different input parameters ("IP1"–"IP5") are identified as crucial for the estimation of the tsunami potential (**Table 2**). As we ultimately aim at (de)selecting lakes for further investigations, depending on the potential for tsunami generation and the potential for consequences of tsunamis, we include both these aspects in the term "tsunami potential." "IP1"–"IP3" focus on the tsunami-generating potential, while "IP4" and "IP5" focus on the tsunami consequences. The five parameters are selected to represent the first-order tsunami potential derived from basic topographical, bathymetrical, and seismological input parameters, due to their simplicity.

IP1: Potential for SAEMM

For the parameterization of the potential for tsunamis generated by SAEMM for each lake, it is important to assess i) the potential for SAEMM that enter the water, and ii) their potential to generate a tsunami. To answer ii), estimations of expected volumes entering the water are crucial. Making statements about likely locations of mass failures requires an understanding of factors and processes relevant for slope instabilities as well as their spatial variability (Fischer et al., 2012). Without knowing the local site conditions, topography is often used as a proxy for potential mass movements (e.g., Coe et al., 2004; Fernandes et al., 2004; Cauzzi et al., 2018). The Fahrböschung (Heim 1932) is defined as

$$\tan \alpha = \frac{H}{L} \tag{3}$$

where H equals the fall height and L the horizontal runout distance. The Fahrböschung can thus be interpreted as the slope angle from the top of a slide to its runout.

Equation 3 is often used to estimate the travel distance of a mass movement, depending on its volume. As the volumes of such potential SAEMM alongshore the investigated lakes are unknown, our model is based on a very simple assumption: Rocks tend to mobilize for Fahrböschung >30° (Gerber, 1994; Heinimann et al., 1998), therefore we calculate the Fahrböschung for each pixel of the SRTM DEM down to its closest point on the shoreline. These calculations are made for each pixel within the watershed around each lake, which we limit to a buffer zone of 5 km around each lake's shoreline (in order not to get very large watersheds in the relatively flat zones of the Swiss Plateau). This value of 5 km corresponds also to the runout distance of the Rossberg landslide, one of the major historic landslides in Switzerland (volume: ~40 Million m^3; Thuro et al., 2006). The input parameter representing the relative tsunami potential posed by SAEMM for each lake (IP1; before normalization) is then estimated by calculating the ratio of pixels with Fahrböschung >30° to the total amount of pixels in the watershed area. Hence, due to the lack of landslide-volume information, we assume here that any potential landslide entering the water may generate a tsunami (which is a conservative assumption). By calculating the Fahrböschung for each pixel of the DEM to the shoreline, potential landslide source zones with locally steep slope inclinations that are too far away from the shoreline (and thus getting a low Fahrböschung value) are not considered as sources of landslides that may reach the lake.

IP2: Potential for SAQMM

The parametrization of the potential for SAQMM is quite simple and straightforward: As subaqueous landslide source areas in Swiss perialpine lakes tend to occur on slopes with inclinations between 10 and 25° (Schnellmann et al., 2006; Hilbe et al., 2011; Strasser et al., 2011; Strupler et al., 2018b), the ratio between the amount of pixels with inclinations between 10 and 25° to the amount of pixels belonging to the lake's slopes (here defined as slope inclinations >5°) is used as input parameter representing the potential for SAQMM (IP2). For the lakes Lugano and Maggiore, which share boundaries with Italy, SwissMap Vector 10/25 data (swisstopo) to interpolate bathymetries is partly not available for the Italian territory (~12% and ~43% of the respective lake's area are not covered; see **Supplementary Table S1**; **Supplementary Figures S1** and **S2**). Therefore, potential SAQMM that may occur in these zones of missing bathymetry data are not considered. The omission of these zones is discussed in *Quality and Limitations of the Relative Tsunami-Potential Classification*.

IP3: Potential for Seismicity

The potential for seismicity at each lake site is given by the seismic hazard levels in terms of elastic 5%-damped Spectral Acceleration at vibration period T = 0.3s − SA(0.3s) for a mean exceedance probability of 10% in 50 years (SuiHaz2015; Wiemer et al., 2016) at each lake center point. The SA(0.3s) values at each lake center were obtained through interpolation of the data of the national Swiss hazard map using ordinary kriging. The seismic hazard values are valid for a reference rock with an average shear-wave velocity of the uppermost 30 m of the soil (Vs_{30}) of 1,100 m/sec. Potential site amplification due to the lake sediments was not considered, as models are still being developed. We did not use Peak Ground Acceleration due to its intrinsic strong saturation with magnitude and distance, that implies comparatively poorer representation of the earthquake sources dominating the hazard at a given location. Mid-to-long period spectral ordinates should be preferred as seismic shaking parameters for the exercise at hand; however, SuiHaz2015 results for T > 1s should be used with caution, as some of the ground motion models used for SuiHaz2015 are better constrained at short and mid periods

(due to the larger number of records used for calibration.) With this background, we finally opted for SA(0.3s), that has the additional advantage of showing a good correlation with macroseismic intensity shaking for damaging events in Switzerland (Panzera et al., under review).

IP4: Inverse Shoreline Development Ratio

It is assumed that for tsunamis occurring in lakes featuring complex shapes with multiple basins, geometric effects could limit the main damage to a single basin. The amount of wave energy transferred around bends also depends on the wave length relative to the lake width. For narrow lakes, long wavelengths can be transmitted without loss of energy (Harbitz, 1992). Oppikofer et al. (2019) state that numerical simulations of SAEMM-induced tsunamis show reductions in wave heights by 30% or more for perpendicular changes in wave direction, which is often the case for fjord-type lakes with multiple basins. To account for the complexity of a lake's shape, an input parameter calculating the inverse of the "shoreline development ratio (SDR)" (Aronow, 1982) is calculated for each lake (IP4). The SDR is calculated from the ratio of the shoreline length for a hypothetical, perfectly circular lake with the same surface area to the actual shoreline length. Higher values mean less complex lake shapes and thus higher potential damage for large parts of the lake shores.

IP5: Inundation Potential

The second parameter related to the tsunami-damage potential (**Table 2**), is called inundation potential (IP5). The assumption made here for parameterization is that low-lying areas (here defined as <5 m above mean lake level) are particularly prone to tsunami inundation. IP5 is obtained by calculating the ratio of the number of pixels that are located in the elevation range from below lake level up to 5 m above lake level to the total amount of pixels within a buffer zone of 1,000 m around the lakeshore. The 1,000 m buffer is arbitrarily chosen, based on modeled inundation distances caused by potential Lake Lucerne landslide-tsunamis (Hilbe and Anselmetti, 2015).

Normalization of the Input Parameters

In order to obtain similar ranges for each IP, each IP is normalized by the range of the values for all lakes (i.e., the minimum value of each IP equals 0 and the maximum value of each IP equals 1). For the IPs that represent ratios (i.e., all IPs except IP3), it is thus important to note that this normalization does not mean that a value of 1 corresponds to a calculated ratio of 100%. Non-normalized IP values can be found in the **Supplementary Table S2**.

Classification

Classification by Main Tsunami Sources

Classification by main tsunami sources (IP1 and IP2) is done with a k-means cluster analysis algorithm (Hartigan and Wong, 1979). The goal of this approach is to construct different lake classes that share common characteristics, i.e., similar combinations of IP1 and IP2 values.

TABLE 3 | Normalized input parameters for each lake.

Index	Name	IP1	IP2	IP3	IP4	IP5
1	L. Geneva	0.02	0.601	0.329	0.286	0.168
2	L. Constance	0.005	0.472	0.019	0.005	0.626
3	L. Maggiore	0.062	0.664	0	0.007	0.114
4	L. Neuchatel	0.002	0.41	0.265	0.282	0.726
5	L. Lucerne	0.207	0.773	0.463	0	0.215
6	L. Zurich	0.009	0.741	0.131	0.01	0.328
7	L. Lugano	0.221	0.651	0.011	0.018	0.052
8	L. Thun	0.072	0.796	0.538	0.319	0.268
9	L. Biel	0.007	0.305	0.223	0.464	0.511
10	L. Zug	0.068	0.819	0.252	0.582	0.288
11	L. Brienz	0.438	0.717	0.533	0.6	0.163
12	L. Walen	0.373	0.812	0.619	0.44	0.123
13	L. Murten	0.005	0.049	0.284	0.954	0.705
14	L. Sempach	0.002	0.226	0.07	0.928	0.549
15	L. Hallwil	0.01	0.681	0.036	0.73	0.36
16	L. Joux	0.018	0.257	0.106	0.397	0.167
17	L. Greifen	0.002	0.121	0.107	0.765	0.687
18	L. Sarnen	0.007	0.687	0.469	0.71	0.255
19	L. Aegeri	0.046	0.732	0.327	0.768	0.198
20	L. Baldegg	0.001	0.594	0.067	0.831	0.508
21	L. Sils	0.177	0.81	0.634	0.532	0.134
22	L. Silvaplana	0.064	0.884	0.686	0.528	0.112
23	L. Kloental	0.68	0.456	0.568	0.57	0
24	L. Pfaeffikon	0	0.227	0.121	0.959	1
25	L. Lauerz	0.053	0	0.447	0.642	0.411
26	L. Lungern	0.258	0.734	0.487	0.524	0.096
27	L. Poschiavo	0.466	0.791	0.59	0.944	0.176
28	L. Oeschinen	1	1	1	1	0.077

Prioritization by Additional Preconditioning Parameters (IP3–IP5)

The lakes in each class are further prioritized by the additional input parameters IP3–IP5. As the tsunami potential for each lake needs to be assessed with regard to a specific purpose, we do the prioritization for each class by sorting it according to IP3–IP5 separately (i.e., we do not aggregate IP3–IP5).

RESULTS

Input parameters for Each Lake

The input parameters for each lake are shown in **Table 3** and their spatial distribution are shown in **Figure 2**.

Table 3 and **Figure 2** show that:

- The highest values of IP1 (SAEMM) are found for alpine lakes Oeschinen, Kloental, Poschiavo, Brienz, and Walen, whereas the lowest values can be found for "Swiss Plateau" lakes Pfaeffikon, Baldegg, Sempach, and Greifen.
- The highest IP2 (SAQMM) values include lakes Oeschinen, Silvaplana, Zug, Walen, and Lake Sils. The lakes with the lowest potential for SAQMM are lakes Lauerz, Murten, Greifen, Sempach, and Pfaeffikon.
- The highest IP3 (seismicity) value is found in Lake Oeschinen, followed by lakes Silvaplana, Sils, Walen, and Poschiavo. The lowest values are found at Italy-bordering lakes Maggiore and Lugano, and at lakes Constance, and Hallwil.

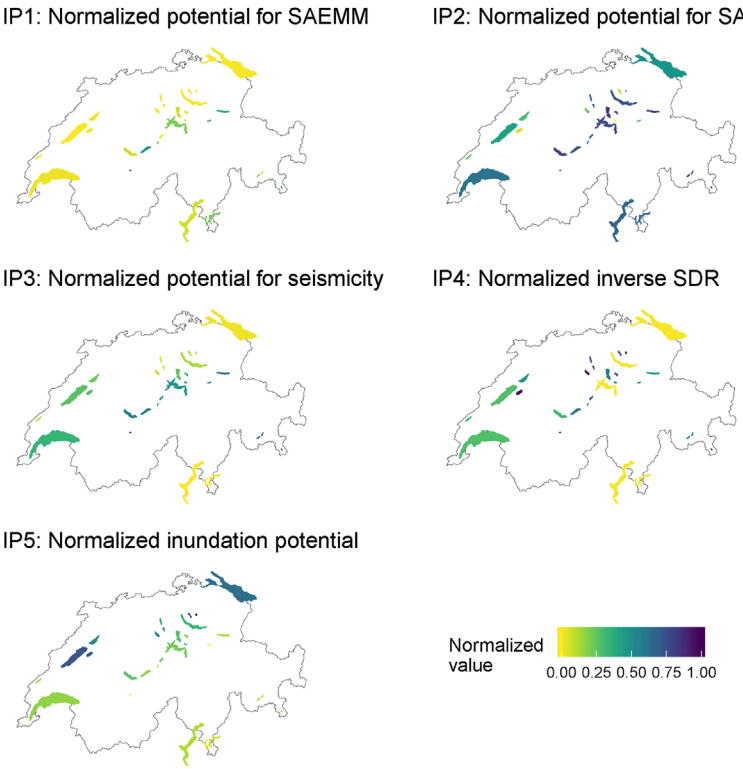

FIGURE 2 | Spatial distribution of the normalized input parameters.

- The highest IP4 (inverse SDR) values are found for lakes Oeschinen, Pfaeffikon, Murten, Poschiavo, and Sempach. All these lakes have simple circular or oval shapes. The lowest values of IP4 are assigned to lakes Lucerne, Constance, Maggiore, and Zurich. These lakes consist of multiple basins, and many of them are visually separated into different branches
- IP5 (inundation potential) is generally higher for alpine-distal lakes than for alpine-proximal lakes, with lake Pfaeffikon having the highest value, followed by lakes Neuchatel, Murten, Greifen, and Constance. The lowest IP5-values are found for lakes Kloental, Lugano, Oeschinen, and Lungern.

Classification Results

Main Tsunami Source Classes

Four different clusters have been created with the k-means clustering algorithm applied to IP1 and IP2 (**Figure 3**): One cluster with a low potential for both SAEMM (IP1) and SAQMM (IP2) ("**class I**," gray, amount (n) = 8), one cluster with a high potential for SAQMM (IP2) but low potential for SAEMM (IP1) ("**class II**," cyan, n = 11), one cluster with a medium potential for SAEMM (IP1) and high potential for SAQMM (IP2) ("**class III**," brown, n = 7), and one cluster with a very high potential for SAEMM (IP1) and high potential for SAQMM (IP2) ("**class IV**," purple, n = 2). No cluster exists for the combination of a high potential of SAEMM (IP1) but low potential of SAQMM (IP2) (**Figure 3**).

The spatial distribution of the lakes, colored according to the identified main tsunami potential classes, is shown in **Figure 4**. Lakes of class I only exist north of the Alps (Swiss Plateau and Jura Mountains). Lakes of class II predominate on the Swiss Plateau, but also occur in the Alps. All class III and IV lakes are located in the Alps.

Prioritization by IP3–IP5

Results of the prioritization of the lakes in classes I-IV (cf. **Figure 4**) according to IP3, IP4, and IP5, respectively (**Table 4**), are shown in the following:

DISCUSSION

The proposed workflow allows for a classification of lakes to be investigated more in depth with regard to the respective tsunami triggers. Although landslide-generated waves are complex hazards (e.g., Bullard et al., 2019), the simple parametrization of inputs contributing to SAEMM and SAQMM-induced tsunamis should facilitate identifying the relative tsunami potential for each lake.

Tsunami Potential on the Investigated Lakes

The definition of four different lake classes according to their main tsunami-source (i.e., SAEMM, SAQMM, or a combination of both) gives a first overview on what potential source to consider for each lake. In the Alps, class III [i.e., medium potential for SAEMM (IP1)

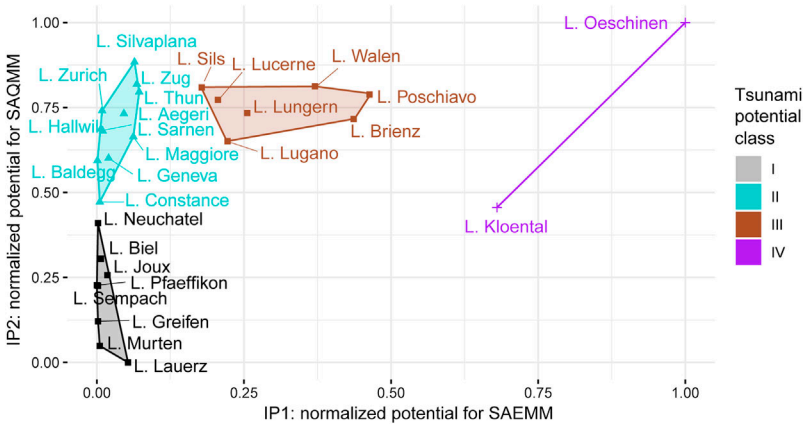

FIGURE 3 | Clusters of lakes according to IP1 and IP2 values, depicting the potential main tsunami potential classes.

and high potential for SAQMM (IP2)] and class IV [i.e., very high potential for SAEMM (IP1) and high potential for SAQMM (IP2)] lakes dominate (**Figures 1**, **4**). Both parameters IP1 and IP2 express the abundance of favourable topographic conditions for mass-movements (i.e., Fahrböschung > 30° for SAEMM and subaquatic slope ranges 10–25° for SAQMM, respectively). The high values of IP1 are related to the fact that many alpine lakes are surrounded by relatively steep slopes. For Lake Oeschinen (**Figure 5**), which is evaluated as having the greatest potential for SAEMM-induced tsunamis, traces of 11 rock-falls that have occurred during the last 2,500 years could be identified at the bottom of the lake (Knapp et al., 2018). The high mean recurrence rate of 200–300 years between the single events supports the high score in our simple model.

Also, the SAEMM-induced tsunamis described in Huber (1982) have occurred in Lake Walen and Lake Lucerne. Both lakes show a relatively high potential for SAEMM (IP1) according to our approach. The comparison of the evaluated potential for SAQMM with documented events show that traces of underwater landslides were found in most of the lakes with a high IP2 score. On the one hand, this can be interpreted as validation of the approach. On the other hand, relatively recent (i.e., younger than a few thousand years) mass movements have decreased the potential for SAQMM occurring in the near future at the same locations, as the slopes need to be re-charged with sediment to become unstable again. It is therefore important for a hazard assessment to further investigate if lakes with historically documented tsunamis that were triggered by SAQMM still have a high potential for such events to recur. However, for comparability reasons between all investigated lakes that build on different dataset qualities (e.g., high-resolution bathymetric and seismic data are not available for all investigated lakes), the history of SAQMM on the lateral slopes is not considered in our simple approach.

The observation that no class for lakes with a high potential for SAEMM but low potential for SAQMM exists, and that lakes closer to the Alps show a generally higher potential for SAQMM,

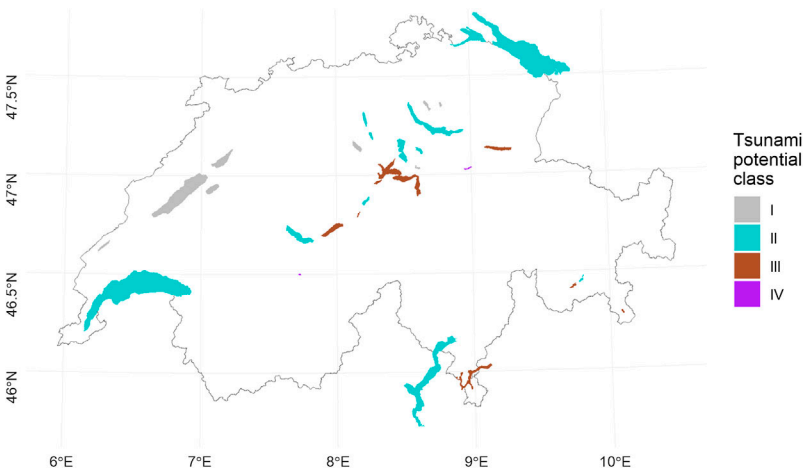

FIGURE 4 | Spatial distribution of the lakes colored according to the identified main tsunami source classes.

TABLE 4 | Prioritization according to IP3 (seismicity, left), IP4 (inverse SDR, middle), and IP5 (inundation potential, right), grouped by main tsunami source classes.

Class	Name	Normalized IP3 (seismicity)	Name	Normalized IP4 (inverse SDR)	Name	Normalized IP5 (inundation potential)
I	L. Lauerz	0.447	L. Pfaeffikon	0.959	L. Pfaeffikon	1.000
	L. Murten	0.284	L. Murten	0.954	L. Neuchatel	0.726
	L. Neuchatel	0.265	L. Sempach	0.928	L. Murten	0.705
	L. Biel	0.223	L. Greifen	0.765	L. Greifen	0.687
	L. Pfaeffikon	0.121	L. Lauerz	0.642	L. Sempach	0.549
	L. Greifen	0.107	L. Biel	0.464	L. Biel	0.511
	L. Joux	0.106	L. Joux	0.397	L. Lauerz	0.411
	L. Sempach	0.070	L. Neuchatel	0.282	L. Joux	0.167
II	L. Silvaplana	0.686	L. Baldegg	0.831	L. Constance	0.626
	L. Thun	0.538	L. Aegeri	0.768	L. Baldegg	0.508
	L. Sarnen	0.469	L. Hallwil	0.730	L. Hallwil	0.360
	L. Geneva	0.329	L. Sarnen	0.710	L. Zurich	0.328
	L. Aegeri	0.327	L. Zug	0.582	L. Zug	0.288
	L. Zug	0.252	L. Silvaplana	0.528	L. Thun	0.268
	L. Zurich	0.131	L. Thun	0.319	L. Sarnen	0.255
	L. Baldegg	0.067	L. Geneva	0.286	L. Aegeri	0.198
	L. Hallwil	0.036	L. Zurich	0.010	L. Geneva	0.168
	L. Constance	0.019	L. Maggiore	0.007	L. Maggiore	0.114
	L. Maggiore	0.000	L. Constance	0.005	L. Silvaplana	0.112
III	L. Sils	0.634	L. Poschiavo	0.944	L. Lucerne	0.215
	L. Walen	0.619	L. Brienz	0.600	L. Poschiavo	0.176
	L. Poschiavo	0.590	L. Sils	0.532	L. Brienz	0.163
	L. Brienz	0.533	L. Lungern	0.524	L. Sils	0.134
	L. Lungern	0.487	L. Walen	0.440	L. Walen	0.123
	L. Lucerne	0.463	L. Lugano	0.018	L. Lungern	0.096
	L. Lugano	0.011	L. Lucerne	0.000	L. Lugano	0.052
IV	L. Oeschinen	1.000	L. Oeschinen	1.000	L. Oeschinen	0.077
	L. Kloental	0.568	L. Kloental	0.570	L. Kloental	0.000

SDR, shoreline development ratio.

may be related to the topographic and geologic predisposition during the glacial excavation of the subsurface: In alpine valleys that are surrounded by steep rock walls, the ice masses were laterally confined and thus the glaciers were thick (Bini et al., 2009), exerting considerable pressure on the substratum, leading to a steep bedrock topography. In contrast, for lakes located on the Swiss Plateau, further from the Alps, the glaciers were able to spread laterally due to the absence of steep rockwalls, which resulted in thinner local ice thicknesses of piedmont-style glaciers, and probably smoother excavations of the bedrock. Certainly, the local geological and geotechnical variability (i.e., relatively soft rocks of the "Molasse" vs. mainly harder rocks of the "Alpine nappes") must have contributed as well to these differences.

FIGURE 5 | Visualization of Lake Oeschinen (Swissimage Orthophoto using base heights of SwissALTI3D: copyright Swisstopo).

On class III/IV lakes, detailed investigations on potential tsunamis generated by SAEMM and SAQMM are recommended. In lakes of class II the potential for SAQMM-generated tsunamis needs to be analyzed more in-depth. For lakes of class I, we do not see an urgent need for further tsunami investigations. Therefore, class I lakes are not considered further in this paper.

Whereas IP1 and IP2 indicate a general predisposition for SAEMM and SAQMM, which was used for the classification into four classes, IP3–IP5 can be used to prioritize between lakes within each class.

The purpose of this study is not to identify and decide on which specific lake should be investigated in more detail, but rather to indicate lakes with a high potential for tsunamis caused by different tsunami sources. The presented results are intended as a guideline for the selection of lakes for further studies, and prioritization of lakes should be based on additional parameters that include IP3–IP5 (**Table 4**), as well as practical considerations (e.g., acquisition time, funding, and inclusion of risk aspects, such as vulnerability and exposure).

- If we assume that most of the mass-movements are triggered seismically, then the prioritization could be made based on IP3 for each class. In this case, lakes that need to be investigated first are lakes Oeschinen, Sils, and Walen for class III and IV, and lakes Silvaplana, Thun, and Sarnen for class II.
- If we focus on whether a potential tsunami could mainly affect single basins and not necessarily entire lakes, then prioritization could be made based on IP4 for each class. In class III/IV, lakes that need to be investigated first in this case are lakes Oeschinen, Poschiavo, and Brienz. In class II, lakes Baldegg, Aegeri, Hallwil, and Sarnen would have priority for further investigations.
- If we focus on the consequences of potential tsunamis, here characterized by the potentially inundated fractions of each lake's shore zone (up to 1 km inland), then the prioritization could be based on IP5 for each class. No lake in class III, which indicates a high potential for SAEMM and SAQMM, has a high inundation potential (IP5). This makes sense, as for a high SAEMM potential (IP1) large parts of the lakeshore needs to be surrounded by a steep topography, which, in turn conflicts with a high inundation potential (IP5), which is parametrized by low-lying areas along the shore. However, lakes in class II (which are characterized by a high potential for SAQMM) that have a relatively high inundation potential are the lakes Constance, Baldegg, and Hallwil. Fortunately, the lakes with the highest inundation potential are the lakes of class I, which do not show a high tsunamigenic potential.

Quality and Limitations of the Relative Tsunami-potential Classification

Due to the limited amount of local site data available for each lake (e.g., no information about expected volumes of potential SAEMM), the nation-wide approach presented here is only based on basic topographical, bathymetrical, and seismological input parameters and thus gives only a broad overview of the relative tsunami potential and main expected triggers. For a full assessment, site-specific geological characteristics (such as acquired for potential SAEMM in Norway; Hermanns et al., 2016) are required. However, despite its simplicity, the method presented here is able to identify lakes with priority for further investigations. Nevertheless, the presented methodology to calculate the various input parameters certainly oversimplifies certain aspects:

- As the volumes of mass movements displacing the water are crucial for the estimation of potential tsunami wave-amplitudes, our simplified methodology is not able to estimate wave heights. At this scale of investigation and with the limited area-wide information available, it is out of scope to assess potential wave heights for each lake, considering the complex interplay between multiple landslide characteristics (see *Background*).
- Additionally, it would be difficult to compare estimated wave heights with the heights documented in historical sources, as, unfortunately, it is rarely documented where and how the waves or their run-up were measured. For assessing the impact at the shore, it is crucial to know whether the wave in the deep water, nearshore, or after shoaling has been described (e.g., Huber, 1980; Fuchs and Boes, 2010).
- Sensitivity analyses showed that the prioritization according to IP3 depends on the selected hazard parameter. If, for example, Peak Ground Acceleration instead of SA(0.3s) is chosen, a few lakes will slightly change positions in the ranking (**Supplementary Figure S60**). This however has no impact on the lakes tsunami classes discussed in the paper. Also, soft sediments, such as occurring on the lake bottom, may amplify seismic shaking considerably. These amplification effects have been neglected in the present study, as consolidated experimental results are not yet available. An ongoing project of the Swiss Seismological Service at Swiss Federal Institute of Technology Zurich is collecting amplification values at the subaqueous slopes and expects them to be remarkably different from those observed onshore.
- To calculate IP5, the ratio of zones lower than 5 m above lake level within the zone of 1 km inland along the shore is calculated. A downside of this approach is that it neglects the micro-topography, e.g., a moraine ridge around the lake may limit the potential inundation, and thus a low-lying area within this shore zone that is located behind such a micro-topographic elevation may contribute to the inundation potential of a lake, but in reality the moraine ridge would hinder the flow (unless overtopping occurred) (c.f. figures in Section 6 of **Supplementary Material**).
- The relatively coarse resolution of the topographic and bathymetric datasets used (SRTM data with 90 m grid resolution) and resampled SwissBathy3D/interpolation from SMV10/25 data (20 m grid resolution) are in our opinion sufficient for such a categorical analysis. Simple tests with a topographic elevation model of better resolution (DHM25) surrounding lakes where existing showed that the relative ranking of the lakes of IP1 did not change.
- The fact that small parts of the SMV 10/25 isobaths of Lakes Lugano and Maggiore are missing on the Italian territory (**Supplementary Figures S1 and S2**) is not expected to change the results of our classification, as the input parameter (IP2) is calculated by the ratio of the pixels with a slope inclination between 10–25° to the total slope area (defined as pixels with inclinations >5°). Both lakes Lugano and Maggiore have a high value of IP2. The missing parts are not likely to lower the IP values considerably, regarding the general morphology of the lakes (**Supplementary Figures S43 and S45**), and their Alpine setting on both the Swiss and Italian side.

The documented historical tsunami events in Swiss perialpine lakes can be used to validate our simplified classification approach. It is worth noting that the historical SAEMM- and SAQMM-tsunami events have occurred on lakes that are evaluated as lakes of classes II and III in our approach, indicating lakes with a high SAQMM- or combined SAEMM- and SAQMM-tsunami potential, with the exception of the

tsunami that occurred on Lake Lauerz (**Table 1**; Bussmann and Anselmetti, 2010 and references therein). According to our classification, Lake Lauerz shows a low tsunamigenic potential posed by SAEMM and SAQMM (and 4). However, the Rossberg landslide significantly changed the lake's shape and size; it has become much smaller with a center further away from the failed mountain slope (Bussmann and Anselmetti, 2010). It would be interesting to compare the tsunami potential for the pre-Rossberg-slide bathymetry to the bathymetry to date and to analyze if the tsunami potential has been reduced. Furthermore, Bussmann and Anselmetti (2010) interpret the tsunami originating from a cascading event, as the mass movement itself did not reach the lake. The subaerial landslide mobilized soft sediments on a swamp plane laterally, which, in turn formed an indenter into the lake causing a tsunami wave. Such cascading effects are not considered in our simplified classification. A cascading effect is also assumed to have caused the AD 563 Tsunami in Lake Geneva (Kremer et al., 2012).

CONCLUSIONS AND OUTLOOK

In this study, a simplified workflow for the classification of the tsunami potential, caused by SAEMM and SAQMM, respectively, in Swiss perialpine lakes, was presented. The results of this study may serve as a starting point for more detailed investigations (e.g., numerical modeling), also considering more field data. Findings show that lakes located within the Alps show generally a higher potential for SAEMM and SAQMM, due to the often steep surrounding rock-walls, and the fjord-type topography of the lake basins with large portions of the lateral slopes lying in the unstable range (i.e., ~10–25°). In contrast, the low lying topography along the shores of the lakes in the Swiss Plateau and Jura Mountains favor inundation caused by potential tsunamis on these lakes. Our results further indicate that all investigated lakes with high potential for SAEMM also have a high potential for SAQMM. The converse is not true, not all lakes with a high potential for SAQMM do have a high potential for SAEMM. We recommend that detailed investigations of the SAQMM-caused tsunami hazard should focus on lakes of classes II–IV (n = 20), and of the SAEMM-caused tsunami hazard on the classes III and IV (n = 9), prioritized by the additional input parameter (IP3–IP5) according to the main purpose of a potential study.

Due to its simplicity, this methodology could also be applied to other lakes worldwide. The minimum of required inputs include digital-elevation raster data, bathymetric raster data, shoreline vector data, and earthquake accelerations. The approach presented herein can be extended by adding further input parameters (e.g., considering cascading hazards). In the context of global warming and thawing of permafrost regions, the parametrization of the potential for subaerial mass-movement may include data extracted from permafrost maps. Furthermore, information about vulnerability and exposure (e.g., degree of building development and type of building) along the shores may be included, when prioritizing specific lakes for more in-depth investigations, especially when considering potential economic damage.

DATA AVAILABILITY STATEMENT

The data analyzed in this study is subject to the following licenses/restrictions: The swisstopo geodata that were used to extract the various Input parameters are copyrighted by swisstopo. However, they can be viewed by everyone for free on maps.geo.admin.ch, but not downloaded. Requests to access these datasets should be directed to the Swiss federal geoportal: maps.geo.admin.ch.

AUTHOR CONTRIBUTIONS

MS: formal analysis, methodology, visualization, and writing—original draft (lead); FE, KK, CC, PB, DV, RB, and DF,: review and editing. FA and SW: funding acquisition, review, and editing.

FUNDING

Funding was received by the Swiss Federal Office for the Environment (FOEN) (17.0092.PJ) and the Swiss National Science Foundation SNSF (171017).

ACKNOWLEDGMENTS

Geodata was used with permission from swisstopo. The authors would like to thank the editor and reviewers for their constructive and helpful comments on this article.

SUPPLEMENTARY MATERIAL

The Supplementary Material for this article can be found online at: https://www.frontiersin.org/articles/10.3389/feart.2020.564783/full#supplementary-material

REFERENCES

Aronow, S. (1982). "Shoreline development ratio," in *Beaches and coastal geology. Encyclopedia of Earth science* (Boston, MA: Springer US), 754–755. doi:10.1007/0-387-30843-1_417

Bini, A., Buoncristiani, J.-F., Couterrand, S., Ellwanger, D., Felber, M., Florineth, D., et al. (2009). *Die Schweiz während des letzteiszeitlichen Maximums (LGM). 1: 500,000*. Köniz, Switzerland: Bundesamt für Landestopografie Swisstopo Wabern.

Bussmann, F., and Anselmetti, F. S. (2010). Rossberg landslide history and flood chronology as recorded in Lake Lauerz sediments (Central Switzerland). *Swiss J. Geosci.* 103, 43–59. doi:10.1007/s00015-010-0001-9

Cauzzi, C., Fäh, D., Wald, D. J., Clinton, J., Losey, S., and Wiemer, S. (2018). ShakeMap-based prediction of earthquake-induced mass movements in Switzerland calibrated on historical observations. *Nat. Hazards* 92, 1211–1235. doi:10.1007/s11069-018-3248-5

Coe, J., Godt, J., Baum, R., Bucknam, R., and Michael, J. (2004). "Landslide susceptibility from topography in Guatemala," in *Landslides: evaluation and stabilization*. Editors W. A. Lacerda, M. M. Ehrlich, S. A. B. Fontura, and A. S. F. Sayão (London, UK: Taylor & Francis Group), 69–78. doi:10.1201/b16816-8

Corella, J. P., Arantegui, A., Loizeau, J. L., DelSontro, T., le Dantec, N., Stark, N., et al. (2014). Sediment dynamics in the subaquatic channel of the Rhone delta (Lake Geneva, France/Switzerland). *Aquat. Sci.* 76, 73–87. doi:10.1007/s00027-013-0309-4

Evers, F. M., Hager, W. H., and Boes, R. M. (2019a). Spatial impulse wave generation and propagation. *J. Waterw. Port Coast. Ocean Eng.* 145, 1–15. doi:10.1061/(ASCE)WW.1943-5460.0000514

Evers, F. M., Heller, V., Fuchs, H., Hager, W. H., and Boes, R. M. (2019b). *Landslide-generated impulse waves in reservoirs: basics and computation. VAW-Mitteilung*. Editor R. M. Boes (Zürich, Switzerland: Versuchsanstalt für Wasserbau, Hydrologie und Glaziologie (VAW), ETH Zürich).

Fabbri, S. C., Herwegh, M., Horstmeyer, H., Hilbe, M., Hübscher, C., Merz, K., et al. (2017). Combining amphibious geomorphology with subsurface geophysical and geological data: a neotectonic study at the front of the Alps (Bernese Alps, Switzerland). *Quat. Int.* 451, 101–113. doi:10.1016/j.quaint.2017.01.033

Fäh, D., Giardini, D., Kästli, P., Deichmann, N., Gisler, M., Schwarz-Zanetti, G., et al. (2011). ECOS-09 earthquake catalogue of Switzerland release 2011. Report and Database. Public catalogue, Zürich, Switzerland, April 17, 2011.

Fanetti, D., Anselmetti, F. S., Chapron, E., Sturm, M., and Vezzoli, L. (2008). Megaturbidite deposits in the Holocene basin fill of Lake Como (Southern Alps, Italy). *Palaeogeogr. Palaeoclimatol. Palaeoecol.* 259, 323–340. doi:10.1016/j.palaeo.2007.10.014

Fernandes, N. F., Guimarães, R. F., Gomes, R. A. T., Vieira, B. C., Montgomery, D. R., and Greenberg, H. (2004). Topographic controls of landslides in Rio de Janeiro: field evidence and modeling. *Catena* 55, 163–181. doi:10.1016/S0341-8162(03)00115-2

Fischer, L., Purves, R. S., Huggel, C., Noetzli, J., and Haeberli, W. (2012). On the influence of topographic, geological and cryospheric factors on rock avalanches and rockfalls in high-mountain areas. *Nat. Hazards Earth Syst. Sci.* 12, 241–254. doi:10.5194/nhess-12-241-2012

Fuchs, H., and Boes, R. (2010). Berechnung felsrutschinduzierter Impulswellen im Vierwaldstättersee. *Wasser Energ. Luft* 102 (3), 215–221. doi:10.3929/ethz-b-000256996

Gerber, W. (1994). "Beurteilung des Prozesses Steinschlag," in *Ganzheitliche Gefahrenbeurteilung. Kursunterlagen FAN-Kurs 1994*. Editors C. Rickli, A. Böll, and W. Gerber (Birmensdorf, Switzerland: Eidgenössische Forschungsanstalt für Wald, Schnee und Landschaft).

Girardclos, S., Schmidt, O. T., Sturm, M., Ariztegui, D., Pugin, A., and Anselmetti, F. S. (2007). The 1996 AD delta collapse and large turbidite in Lake Brienz. *Mar. Geol.* 241, 137–154. doi:10.1016/j.margeo.2007.03.011

Gisler, M., and Fäh, D. (2011). *Grundlagen des Makroseismischen Erdbebenkatalogs der Schweiz*. Zürich, Switzerland: Schweizerischer Erdbebendienst/VDF Hochschulverlag AG). doi:10.3218/3407-3

Glimsdal, S., L'Heureux, J.-S., Harbitz, C. B., and Løvholt, F. (2016). The 29th January 2014 submarine landslide at Statland, Norway-landslide dynamics, tsunami generation, and run-up. *Landslides* 13, 1435–1444. doi:10.1007/s10346-016-0758-7

Glimsdal, S., Pedersen, G. K., Harbitz, C. B., and Løvholt, F. (2013). Dispersion of tsunamis: does it really matter? *Nat. Hazards Earth Syst. Sci.* 13, 1507–1526. doi:10.5194/nhess-13-1507-2013

Hafsteinsson, H. J., Evers, F. M., and Hager, W. H. (2017). Solitary wave run-up: wave breaking and bore propagation. *J. Hydraul. Res.* 55, 787–798. doi:10.1080/00221686.2017.1356756

Hager, W. H., and Evers, F. M. (2020). Impulse waves in reservoirs: research up to 1990. *J. Hydraul. Eng.* 146, 1–13. doi:10.1061/(ASCE)HY.1943-7900.0001770

Harbitz, C. B. (1992). Tech. Rep. 6. Reflection-transmission of nonlinear waves in channel bends. Oslo, Norway: Institute of Mathematics, University of Oslo.

Hartigan, J. A., and Wong, M. A. (1979). Algorithm as 136: a K-means clustering algorithm. *J. Appl. Stat.* 28, 100. doi:10.2307/2346830

Heim, A. (1932). *Bergsturz und Menschenleben. Beiblatt zur Vierteljahrsschrift der Naturforschenden Gesellschaft in Zürich*. Zürich, Switzerland: Beer & Co. Vol. 77, Issue 20.

Heinimann, H. R., Hollenstein, K., Kienholz, H., Krummenacher, B., and Mani, P. (1998). *Methoden zur Analyse und Bewertung von Naturgefahren*. Bern, Switzerland: Bundesamt für Umwelt, Wald und Landschaft (BUWAL). Umwelt-Materialien Naturgefahren 85, 248.

Heller, V., and Hager, W. H. (2010). Impulse product parameter in landslide generated impulse waves. *J. Waterw. Port Coast. Ocean Eng.* 136, 145–155. doi:10.1061/(ASCE)WW.1943-5460.0000037

Heller, V., and Hager, W. (2014). A universal parameter to predict subaerial landslide tsunamis? *J. Marine. Sci. Eng.* 2, 400–412. doi:10.3390/jmse2020400

Heller, V., Hager, W. H., and Minor, H.-E. (2008). Scale effects in subaerial landslide generated impulse waves. *Exp. Fluid* 44, 691–703. doi:10.1007/s00348-007-0427-7

Henriod, S., Douard, R., Ullmann, D., and Humbel, R. (2016). *Statistik der Bevölkerung und Haushalte (STATPOP)*. BFS-Nummer: be-d-00.03-13-STATPOP-v16. Bern, Switzerland: Bundesamt für Statistik (BFS).

Hermanns, R. L., Oppikofer, T., Anda, E., Blikra, L. H., Böhme, M., and Bunkholt, H. (2012). NGU Rep. 2012.029, 49. Recommended hazard and risk classification system for large unstable rock slopes in Norway. Available at: http://www.ngu.no/no/hm/Publikasjoner/Rapporter/2012/2012-029/ (Accessed April 16, 2020).

Hermanns, R. L., Oppikofer, T., Anda, E., Blikra, L. H., Böhme, M., and Bunkholt, H. (2013). Hazard and risk classification for large unstable rock slopes in Norway. *Ital. J. Eng. Geol. Environ.* 6, 245–254. doi:10.4408/IJEGE.2013-06.B-22

Hermanns, R. L., Oppikofer, T., Böhme, M., Dehls, J., Molina, F., and Penna, I. (2016). Rock slope instabilities in Norway: first systematic hazard and risk classification of 22 unstable rock slopes from northern, western and southern Norway. *Landslides Eng. Slopes Exp. Theory Pract.* 2, 1107–1114. doi:10.1201/b21520-133

Hilbe, M., and Anselmetti, F. S. (2014). Signatures of slope failures and river-delta collapses in a perialpine lake (Lake Lucerne, Switzerland). *Sedimentology* 61, 1883–1907. doi:10.1111/sed.12120

Hilbe, M., and Anselmetti, F. S. (2015). Mass movement-induced tsunami hazard on perialpine Lake Lucerne (Switzerland): scenarios and numerical experiments. *Pure Appl. Geophys.* 172, 545–568. doi:10.1007/s00024-014-0907-7

Hilbe, M., Anselmetti, F. S., Eilertsen, R. S., Hansen, L., and Wildi, W. (2011). Subaqueous morphology of Lake Lucerne (Central Switzerland): implications for mass movements and glacial history. *Swiss J. Geosci.* 104, 425–443. doi:10.1007/s00015-011-0083-z

Huber, A. (1980). *Schwallwellen in seen als Folge von Felsstürzen. VAW-Mitteilung*. Editor D. Fischer (Zürich, Switzerland: Versuchsanstalt für Wasserbau, Hydrologie und Glaziologie, ETH Zürich).

Huber, A. (1982). Felsbewegungen und Uferabbrüche an Schweizer Seen, ihre Ursachen und Auswirkungen. *Eclogae Geol. Helv.* 75, 563–578. doi:10.5169/seals-165242

Jarvis, A., Reuter, H. I., Nelson, E. G., and Guevara, E. (2008). Hole-filled SRTM for the globe version 4, available from the CGIAR-CSI SRTM 90m database. Available at: http://srtm.csi.cgiar.org (Accessed March 16, 2020).

Knapp, S., Gilli, A., Anselmetti, F. S., Krautblatter, M., and Hajdas, I. (2018). Multistage rock-slope failures revealed in lake sediments in a seismically active Alpine region (Lake Oeschinen, Switzerland). *J. Geophys. Res. Earth Surf.* 123, 658–677. doi:10.1029/2017JF004455

Kremer, K., Hilbe, M., Simpson, G., Decrouy, L., Wildi, W., and Girardclos, S. (2015). Reconstructing 4,000 years of mass movement and tsunami history in a deep peri-Alpine lake (Lake Geneva, France-Switzerland). *Sedimentology* 62, 1305–1327. doi:10.1111/sed.12190

Kremer, K., Simpson, G., and Girardclos, S. (2012). Giant Lake Geneva tsunami in ad 563. *Nat. Geosci.* 5, 756–757. doi:10.1038/ngeo1618

Kremer, K., Wirth, S. B., Reusch, A., Fäh, D., Bellwald, B., Anselmetti, F. S., et al. (2017). Lake-sediment based paleoseismology: limitations and perspectives from the Swiss Alps. *Quat. Sci. Rev.* 168, 1–18. doi:10.1016/j.quascirev.2017.04.026

Løvholt, F., Pedersen, G., Harbitz, C. B., Glimsdal, S., and Kim, J. (2015). On the characteristics of landslide tsunamis. *Phil. Trans. R. Soc. A* 373, 20140376. doi:10.1098/rsta.2014.0376

Monecke, K., Anselmetti, F. S., Becker, A., Sturm, M., and Giardini, D. (2004). The record of historic earthquakes in lake sediments of Central Switzerland. *Tectonophysics* 394, 21–40. doi:10.1016/j.tecto.2004.07.053

Nadim, F., Kalsnes, B., and Eide, A. (1996). "Analysis of submarine slope stability under seismic action," in *Landslides*. Editor K. Senneset (Rotterdam, Netherlands: Balkema), 561–565.

Oppikofer, T., Hermanns, R. L., Roberts, N. J., and Böhme, M. (2019). SPLASH: semi-empirical prediction of landslide-generated displacement wave run-up heights. *Geol. Soc. Spec. Publ.* 477, 353–366. doi:10.1144/SP477.1

Reusch, A. (2015). Sublacustrine paleoseismology and fluid flow in the Western Swiss Molasse basin: new constraints from the sedimentary archive of Lake Neuchâtel. PhD Thesis. Zurich, Switzerland: ETH Zurich, Nr. 232131.

Roberts, N. J., McKillop, R. J., Lawrence, M. S., Psutka, J. F., Clague, J. J., and Brideau, M.-A. (2013). "Impacts of the 2007 landslide-generated tsunami in Chehalis Lake, Canada," in *Landslide science and practice*. Editors C. Margottini, P. Canuti, and K. Sassa (Berlin, Germany and Heidelberg, Germany: Springer), 133–140. doi:10.1007/978-3-642-31319-6_19

Romstad, B., Harbitz, C. B., and Domaas, U. (2009). A GIS method for assessment of rock slide tsunami hazard in all Norwegian lakes and reservoirs. *Nat. Hazards Earth Syst. Sci.* 9, 353–364. doi:10.5194/nhess-9-353-2009

Schnellmann, M., Anselmetti, F. S., Giardini, D., and McKenzie, J. A. (2006). 15,000 years of mass-movement history in Lake Lucerne: implications for seismic and tsunami hazards. *Eclogae Geol. Helv.* 99, 409–428. doi:10.1007/s00015-006-1196-7

Schnellmann, M., Anselmetti, F. S., Giardini, D., McKenzie, J. A., and Ward, S. N. (2002). Prehistoric earthquake history revealed by lacustrine slump deposits. *Geology* 30, 1131–1134. doi:10.1130/0091-7613(2002)030<1131:PEHRBL>2.0.CO;2

Siegenthaler, C., Finger, W., Kelts, K., and Wang, S. (1987). Earthquake and seiche deposits in Lake Lucerne, Switzerland. *Eclogae Geol. Helv.* 80, 241–260.

Siegenthaler, C., and Sturm, M. (1991). Slump induced surges and sediment transport in Lake Uri, Switzerland. *SIL Proc. 1922–2010* 24, 955–958. doi:10.1080/03680770.1989.11898889

Strasser, M., Hilbe, M., and Anselmetti, F. S. (2011). Mapping basin-wide subaquatic slope failure susceptibility as a tool to assess regional seismic and tsunami hazards. *Mar. Geophys. Res.* 32, 331–347. doi:10.1007/s11001-010-9100-2

Strasser, M., Monecke, K., Schnellmann, M., and Anselmetti, F. S. (2013). Lake sediments as natural seismographs: a compiled record of Late Quaternary earthquakes in Central Switzerland and its implication for Alpine deformation. *Sedimentology* 60, 319–341. doi:10.1111/sed.12003

Strasser, M., Stegmann, S., Bussmann, F., Anselmetti, F. S., Rick, B., and Kopf, A. (2007). Quantifying subaqueous slope stability during seismic shaking: Lake Lucerne as model for ocean margins. *Mar. Geol.* 240, 77–97. doi:10.1016/j.margeo.2007.02.016

Strupler, M., Anselmetti, F. S., Hilbe, M., Kremer, K., and Wiemer, S. (2020). A workflow for the rapid assessment of the landslide-tsunami hazard in peri-alpine lakes. *Geol. Soc. Spec. Publ.* 500, 81–95. doi:10.1144/SP500-2019-166

Strupler, M., Anselmetti, F. S., Hilbe, M., and Strasser, M. (2018a). Quantitative characterization of subaqueous landslides in Lake Zurich (Switzerland) based on a high-resolution bathymetric dataset. *Geol. Soc.Spec. Publ.* 477, 399–412. doi:10.1144/SP477.7

Strupler, M., Danciu, L., Hilbe, M., Kremer, K., Anselmetti, F. S., Strasser, M., et al. (2018b). A subaqueous hazard map for earthquake-triggered landslides in Lake Zurich, Switzerland. *Nat. Hazards* 90, 51–78. doi:10.1007/s11069-017-3032-y

Strupler, M., Hilbe, M., Anselmetti, F. S., Kopf, A. J., Fleischmann, T., and Strasser, M. (2017). Probabilistic stability evaluation and seismic triggering scenarios of submerged slopes in Lake Zurich (Switzerland). *Geo Mar. Lett.* 37, 241–258. doi:10.1007/s00367-017-0492-8

Strupler, M., Hilbe, M., Kremer, K., Danciu, L., Anselmetti, F. S., Strasser, M., et al. (2018c). Subaqueous landslide-triggered tsunami hazard for Lake Zurich, Switzerland. *Swiss J. Geosci.* 111, 353. doi:10.1007/s00015-018-0308-5

Tappin, D. R., Watts, P., and Grilli, S. T. (2008). The Papua New Guinea tsunami of 17 July 1998: anatomy of a catastrophic event. *Nat. Hazards Earth Syst. Sci.* 8, 243–266. doi:10.5194/nhess-8-243-2008

Thuro, K., Berner, C., and Eberhard, E. (2006). Der Bergsturz von Goldau 1806 - was wissen wir 200 Jahre nach der Katastrophe? *Bull. Angew. Geol.* 11, 13–24.

Ward, S. N. (2001). Landslide tsunami. *J. Geophys. Res.* 106, 11201–11215. doi:10.1029/2000jb900450

Watts, P., Grilli, S. T., Tappin, D. R., and Fryer, G. J. (2005). Tsunami generation by submarine mass failure. II: predictive equations and case studies. *J. Waterw. Port Coast. Ocean Eng.* 131, 298–310. doi:10.1061/(asce)0733-950x(2005)131:6(298)

Wiemer, S., Danciu, L., Edwards, B., Marti, M., Fäh, D., and Hiemer, S. (2016). Seismic hazard model 2015 for Switzerland. 1–163. doi:10.12686/a2

Wirth, S. B., Girardclos, S., Rellstab, C., and Anselmetti, F. S. (2011). The sedimentary response to a pioneer geo-engineering project: tracking the Kander River deviation in the sediments of Lake Thun (Switzerland). *Sedimentology* 58, 1737–1761. doi:10.1111/j.1365-3091.2011.01237.x

Conflict of Interest: The authors declare that the research was conducted in the absence of any commercial or financial relationships that could be construed as a potential conflict of interest.